Gypsum speleothems in lava tubes from Lanzarote (Canary Islands). Ion sources and pathways

Pedro Huerta [a,*], Andrea Martín-Pérez [b], Rebeca Martín-García [c,d], Álvaro Rodríguez-Berriguete [d,e], Ángel La Iglesia Fernández [e], Ana María Alonso-Zarza [d,e]

[a] Departamento de Geología, Escuela Politécnica Superior de Ávila, Universidad de Salamanca, avda. Hornos Caleros, 50, 05003 Ávila, Spain
[b] Institute of Palaeontology ZRC SAZU, Novi trg 2, SI 1000 Ljubljana, Slovenia
[c] Station d'Ecologie Théorique et Expérimentale - UMR 5321 CNRS, 09200 Moulis, France
[d] Departamento de Mineralogía y Petrología, Facultad de Ciencias Geológicas, Universidad Complutense de Madrid, c/José Antonio Novais, 2, 28040 Madrid, Spain
[e] Instituto de Geociencias, IGEO (CSIC, UCM), c/José Antonio Novais, 2, 28040 Madrid, Spain

ARTICLE INFO

ABSTRACT

Lava tubes from Lanzarote Island in the Canary Archipelago commonly show white speleothems that stand out from the black basaltic rock. Mineralogical analyses of the speleothems from El Covón and Chifletera lava tubes show that gypsum is the dominant mineral with minor amounts of halite. Speleothems composed of microcrystalline gypsum (up to 150 μm long) are: coatings, globules, or extensive white powder accumulations covering the tube floor. Those composed of macrocrystalline gypsum with millimetric-size tabular and lenticular crystals are: crusts and stalactites. Uranium series dating of speleothems show ages ranging from 6217 ± 1644 yr to $40{,}039 \pm 4748$ yr. $\delta^{34}S$ and the $\delta^{18}O$ of gypsum speleothems ($\delta^{34}S$ is 20.97‰ V-CDT and $\delta^{18}O$ is 9.78‰ V-SMOW) is similar to that of sulphate dissolved in seawater. $^{87}Sr/^{86}Sr$ from speleothems (0.708665–0.708976) suggests that the main source of Ca is seawater, but additional Ca contributions from aeolian dust have reduced the Sr isotope values. These data support the idea that gypsum precipitates in the lava tube by evaporation of marine spray or solutions derived from marine spray. Two probable vias for ions input into the lava tube are considered: 1) sea spray circulating through the lava tube; 2) low-frequency rain infiltration leaching the marine spray salts precipitated at the surface. The constant supply of ions from sea spray, air currents in the cave, and the fast, but partial, evaporation due to the high relative humidity in the lava tube favours accumulation of major amounts of gypsum and subordinately halite. Scarcity of precipitation in the western Canary Islands prevents dissolution of gypsum speleothems.

© 2019 Elsevier B.V. All rights reserved.

1. Introduction

Gypsum, identified in numerous caves around the world (Hill and Forti, 1997), is considered the second most abundant cave mineral after calcite (Onac, 2012). Gypsum speleothems are predominant in gypsum karstic caves in arid climates (Calaforra et al., 2008), where they form by evaporation (Gázquez et al., 2011). In limestone caves SO_4^{2-} is supplied by the oxidation of pyrite or other sulphides, oxidation of H_2S or by dissolution of interbedded evaporites in the limestone (Hill and Forti, 1997). Gypsum deposits replacing calcite in limestone caves constitute one of the main features of sulphuric acid speleogenesis (Galdenzi and Menichetti, 1995; Polyak and Provencio, 2001; Palmer, 2013). In volcanic caves such as lava tubes, gypsum is also considered one of the most abundant minerals (Forti, 2005) but very few studies provide detailed description of gypsum speleothems in these settings

(Jakobsson et al., 1992; White, 2010), particularly regarding their geochemistry (Dillon et al., 2009; LaPointe et al., 2013).

There are few processes involving sulphate precipitation in volcanic settings (Hill and Forti, 1997; Onac and Forti, 2011): 1) processes related to high temperatures during early stages of lava tube formation, such as sublimation from fumarole gases or solubilization of previously formed minerals interacting with water; 2) low temperature processes like bat guano alteration or infiltration of sulphate-enriched meteoric waters.

The study of sulphur isotopes ($\delta^{34}S$) and $^{87}Sr/^{86}Sr$ ratios have been used to identify the ion sources for gypsum in caves in different settings around the world, such as the quartz-sandstone caves in the Gran Sabana region, Venezuela (Sauro et al., 2014), the deep caves of Nullarbor Plain, Australia (Lipar et al., in press), caves from Cerna Valley in Romania, coastal caves of the Bahamas (Bottrell et al., 1993; Onac et al., 2009) and lava tubes of New Mexico (Dillon et al., 2009; LaPointe et al., 2013).

An important number of lava tubes in the Lanzarote Island (i.e. Covón/Chifletera, Esqueleto, Prendes, etc.) contain abundant gypsum speleothems covering walls and floors. This work aims to: 1) characterize

* Corresponding author.
  E-mail address: phuerta@usal.es (P. Huerta).

the mineralogy and petrography of all varieties of gypsum speleothems; 2) identify calcium and sulphate sources and pathways and 3) understand the processes of speleothem formation. This study contributes to the understanding of the formation and preservation processes that have favoured the decimetric accumulations of gypsum. While these speleothems are rather common in other lava tubes, they have not been widely described in the literature.

2. Geological settings

Lanzarote, the northern and easternmost island of the volcanic Canary Archipelago, about 100 km from the African coast (Fig. 1), is considered, along with Fuerteventura, as the oldest and lowest relief islands of the Canaries. Volcanic eruptions in the last 300 years in Lanzarote are Timanfaya, 1730–1736 and Tinguatón and Chinero, 1824 (Carracedo et al., 1992; Criado et al., 2013). Rocks in Lanzarote are mainly composed of basalts, although aeolian sediments and elevated marine deposits appear also close to the coast (Zazo et al., 2002). Lanzarote has a highly eroded landscape with deep-incised valleys and wide low-relief areas with major calcrete development (Alonso-Zarza and Silva, 2002; Alonso-Zarza et al., 2016).

Lanzarote preserves an important number of lava tubes formed during various eruptions. Some of them host gypsum speleothems (Smith, 2015). One of the most famous is the Corona volcano lava tube (7.6 km long), which can be visited at the Cueva de los Verdes in the north eastern part of the island (Carracedo et al., 2003). Others occur in Middle Pleistocene lavas from the western part of Lanzarote, like the Covón and Chifletera lava tubes, as well as those identified in the 1730–1736 lavas (Gómez-Ortiz et al., 2014). Covón and Chifletera are the names of two lava tubes located in the same sector (Fig. 1). In this study we used the names given by the personnel of the National Park to avoid confusion with different names and locations indicated in different publications (Serantes Vergara and Pena Muiño, 2013b, a; Smith, 2015). The entrance of Covón (Coordinates UTM 28N, ETRS 89, X: 613973; Y: 3208135) (also called Pardelas), is located 40 m from the shore at the top of a 30 m high cliff, and Chifletera (Coordinates UTM 28N, ETRS 89, X: 614241; Y: 3207920) has its entrance 400 m inland, at 50 m above sea level. Its sea entrance (Coordinates UTM 28N, ETRS 89, X: 613836; Y: 3207914) opens at 15 m in a 25 m high cliff (Fig. 1). These lava tubes are located in the Timanfaya National Park, which limits tourist visits, favouring their protection.

Climate in Lanzarote is dominated by the scarcity of rainfall (105 mm of mean annual) and warm temperatures that range from 17° to 25 °C as mean minimum and maximum, respectively. Marine trade winds influence the Canary islands during most of the year, although the low relief of Lanzarote and Fuerteventura do not exert any orographic effect. Rainfall is very scarce in comparison with islands of higher relief. Canary Islands receive major amounts of Saharan dust (quartz, limestone fragments, etc.) (Coudé-Gaussen et al., 1987; Menéndez et al., 2007; Criado et al., 2012) brought by African winds related to the Saharan Air Layer (SAL) (Prospero and Lamb, 2003).

3. Methodology

Speleothem samples were collected from two lava tubes. 1) In Covón-Pardelas, samples and environmental parameters were obtained in the same area, about 60 m from the entrance. 2) In Chifletera, samples were recovered within the 200 m from the inland entrance of the lava tube. Environmental parameters were measured in the same area (Fig. 1).

Bulk mineralogy of 20 samples of speleothems was studied using X-ray diffraction (XRD). Patterns were obtained from powder mounts using a Philips semiautomatic PW 1710 diffractometer with monochromatized CuKα radiation. Semiquantitative analyses were performed using EVA software by Bruker (DIFFRAC^{Plus} 2006 version).

Conventional optical petrography was performed on thin sections. Due to their fragility, the speleothems were embedded in Epofer EX 401 and Epofer E 432 resin in a vacuum system before cutting and polishing.

X-ray fluorescence (XRF) analysis was conducted on 11 samples of various speleothems using the Aχios spectrometer from PANalyticalthe LTD, in the facilities of the Universidad Complutense de Madrid.
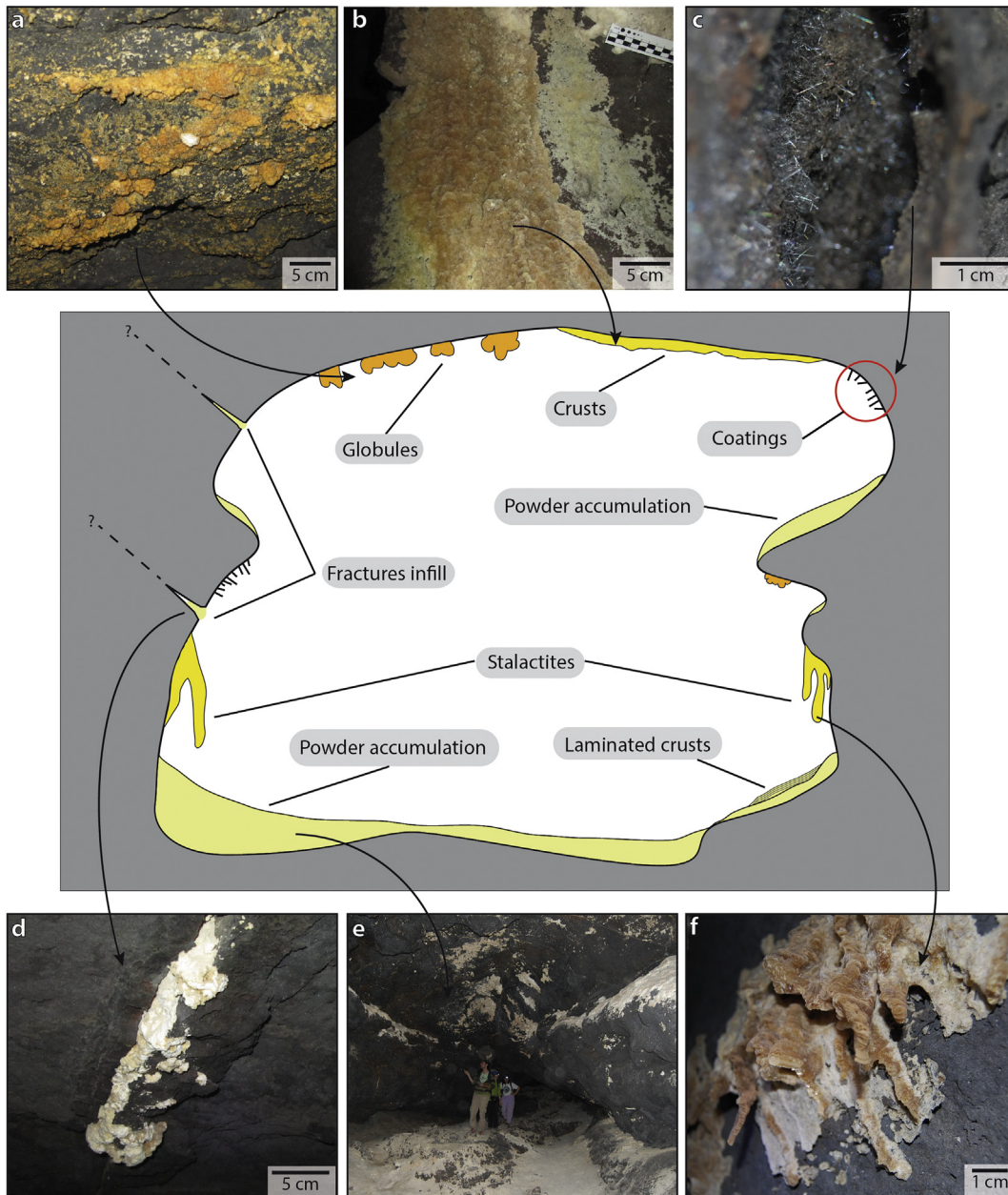
Specimens were examined on a JEOL JSM-IT100 scanning electron microscope (SEM) at the Institute of Palaeontology ZRC SAZU, Ljubljana and at the Museo de Ciencias Naturales de Madrid under a FEI INSPECT scanning electron microscope. Uncoated specimens were observed and photographed in low-vacuum mode (40 Pa) with an accelerating voltage of 15 kV, 20 kV, and 30 kV at a working distance of 9 to 11 mm. Photomicrographs were taken in shadow backscattered electron imaging mode (BSE). Qualitative and semi-quantitative Energy Dispersive X-ray Spectroscopy analysis (EDS) was performed under the same low-vacuum (LV) conditions.

The $^{34}S/^{32}S$ and $^{18}O/^{16}O$ ratios of gypsum sulphate (10 samples) were analysed at the Serveis Cientificotècnics of the Universitat de Barcelona. Samples were first dissolved with deionized water, then filtered and precipitated as $BaSO_4$. Mass spectrometer SO_2 analysis was carried out with a TC/EA DELTA PLUS XP THERMOFISHER mass spectrometer. Reproducibilities were calculated using international and internal laboratory standards systematically interspersed in the analytical batches: 0.2‰ for $\delta^{34}S$ and 0.6‰ for $\delta^{18}O$.
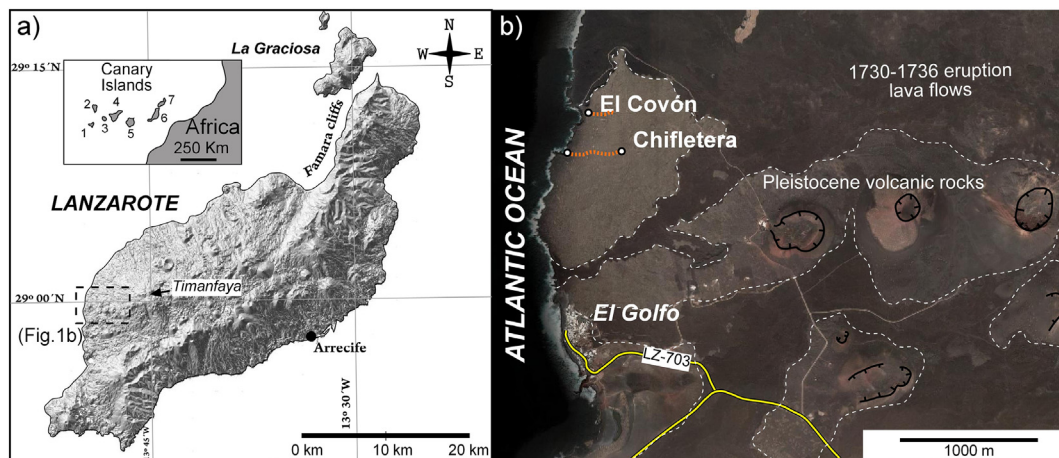
Fig. 1. Map showing location of Lanzarote Island and lava tubes studied. a) General map. Numbers refer to: 1. El Hierro, 2. La Palma, 3. La Gomera, 4. Tenerife, 5. Gran Canaria, 6. Fuerteventura, 7 Lanzarote. b) Orthophoto indicating position, and approximate trace of Covón and Chifletera. White dashed line marks the boundary between 1730-1736 eruption lava flows and Pleistocene volcanics.

$^{87}Sr/^{86}Sr$ isotope ratio was measured at the Geochronology and Isotope Geochemistry facility of the Universidad Complutense de Madrid using a VG TIMS mass spectrometer. Samples were dissolved in 2.5 N HCl, centrifuged and then evaporated. Residue was again dissolved in 2.5 N HCl. The analytical precision for $^{87}Sr/^{86}Sr$ analysis is 0.01‰ (referred to standard NBS-987).

Uranium-series analyses of gypsum crusts and stalactites were performed at the Radiogenic Isotope Laboratory of the University of New Mexico following the method described in Asmerom et al. (2010). Powdered samples were dissolved in 15 N HNO_3 spiked with a mixed solution of ^{229}Th, ^{233}U, and ^{236}U. After that, the subsamples were dissolved in 7 N HNO_3 and U and Th were separated, to be analysed using Thermo Neptune multicollector ICP-MS.

To measure the wind velocity we used a Kestrel 5500 weather meter with a resolution of 0.1 m/s. Humidity and temperature were measured with a HOBO MX2301 Temperature/RH data logger with a resolution for temperature of 0.04 °C and accuracy of ±0.2 °C from 0 to 70 °C and a 0.05% RH resolution and accuracy of ±2.5% from 10% to 90% (typical) to a maximum of ±3.5% including hysteresis at 25 °C (77 °F); below 10% RH and above 90% RH: ±5% typical.

4. Main characteristics of the lava tubes

Lava tubes are dry, without water ponds nor drops on the walls or roofs. The host rock is impervious basalt whose randomly oriented fractures cut the lava tubes from base to top. The width of the fractures varies from millimeters to 3 cm. Most of them are dry and can be filled with gypsum. Temperature and relative humidity measured in Covón are more variable and more sensitive to external temperature changes than those measured in Chifletera.

Covón (Pardelas) has a wide entrance at the top of a cliff with roof collapse that produces another opening close to the entrance. The roof is 2 m thick around the entrance, with multiple roof collapses and is probably thicker inland. The sections are about 7 m wide by 4 m high. Relative humidity in Covón is about 50–70% and temperature varies from 16 °C to 19 °C.

Chifletera has a 2.5 m wide by 1.5 m high entrance at the sea cliff and an inland of 0.5 by 0.5 m. The distance from the cave roof to the surface is about 5–10 m. The size and shape of sections varies along Chifletera lava tube length. Some parts are 8 m wide by 4 m high and others reduce to 2.5 m wide by 1.5 m high. Air currents move from the sea entrance to the inland entrance with air speeds that vary from 0.6 to 2.4 m/s. Mean annual temperature is 19 °C and the average relative humidity 62%; daily variations are <1 °C and a 2%, respectively. Evidence of water percolating during intense rain episodes were found in one fracture in Chifletera, where the gypsum powder accumulated was dissolved on the floor. Only at the sea cliff entrance are salty water drops on walls and roof of this lava tube, as well as halite crystals.

5. Characterization of speleothems

According to XRD and EDS analyses of individual crystals performed during SEM observation, all the speleothems from Covón and Chifletera lava tubes are composed of gypsum and minor amounts of halite (Table 1).

Gypsum speleothems are of two types: microcrystalline, and macrocrystalline. Their detailed description follows, when possible, the terminology used by Hill and Forti (1997) (Fig. 2).

5.1. Microcrystalline gypsum

It is composed of euhedral crystals around 5 μm thick and up to 150 μm long which show flattened morphologies varying from bladed to platy habits. These crystals form loose aggregates and according to their occurrence in different parts of the lava tubes we have distinguished the following types.

5.1.1. Powder accumulations

These are fine white powder deposits that cover most parts of the floor and large areas of walls in both lava tubes, although they are especially abundant in Chifletera. They can pile up to several cm, appearing as dust or snow accumulations. In areas of the lava tube close to entrances,

Table 1
Mineralogical, isotopic composition, and XRF analyses in % mol oxides of speleothems found in Covón/Pardelas (PAR) Chifletera (CHI) lava tubes. G%: gypsum, H%: halite.

Sample	DRX		$^{87}Sr/^{86}Sr$	$\delta^{18}O$	$\delta^{34}S$	% mol oxides																Speleothem
	G %	H %		‰ VSMOW	‰VCDT	CaO	SO_3	Na_2O	Cl	MgO	Al_2O_3	TiO_2	MnO	Fe_2O_3	NiO	SrO	K_2O	SiO_2	P_2O_5	Br	
PAR-1	95	5	0.708892	9.85	21.1	51.59	43.47	1.30	2.33	0.33	0.07	0.01	0.00	0.04	0.00	0.08	0.02	0.38	0.37	0.00	Powder
PAR-2		100																			Coating
PAR-3	91	9		9.75	21.0																Globules
PAR-4	94	6	0.708861	10.31	21.7	50.51	41.27	1.37	3.19	1.21	0.23	0.06	0.01	0.20	0.00	0.06	0.09	1.40	0.39	0.01	Powder
PAR-5	96	4	0.708930			52.78	44.07	0.44	0.61	0.62	0.15	0.03	0.00	0.07	0.00	0.12	0.03	0.68	0.39	0.01	Powder
PAR-8	100		0.708976			52.99	43.36	0.54	1.25	0.70	0.06	0.00	0.00	0.04	0.00	0.18	0.03	0.46	0.39	0.00	Crust
PAR-9	85	15																			Powder
PAR-10	90	10																			Powder
PAR-11	100																				Stalact
PAR-12	100																				Crust
CHI-1	25	15		9.98	20.8																Sand
CHI-2	100			9.12	20.7																Globules
CHI-3	100		0.708924			54.47	43.82	0.00	0.42	0.36	0.04	0.00	0.00	0.02	0.00	0.18	0.02	0.19	0.48	0.00	Globules
CHI-4			0.708912			53.30	44.46	0.00	0.34	0.28	0.00	0.00	0.00	0.02	0.00	0.14	0.02	0.94	0.49	0.00	Stalact
CHI-5	100			9.87	20.7																Stalact
CHI-6	94	6	0.708782	9.62	20.9	25.58	21.30	13.68	38.54	0.25	0.03	0.00	0.00	0.01	0.00	0.02	0.01	0.19	0.37	0.01	Powder
CHI-6 B	49	51																			Powder
CHI-7	90	10																			Powder
CHI-8	94	6	0.708665	10.43	21.1	53.93	42.89	0.63	1.66	0.31	0.00	0.00	0.00	0.00	0.00	0.03	0.02	0.14	0.40	0.00	Powder
CHI-9	88	12		9.47	20.9																Powder
CHI-10.1	100			9.41	20.9																Globules
CHI-10.2	100																				Globules
CHI-11	100					53.72	44.65	0.00	0.63	0.25	0.00	0.00	0.00	0.02	0.00	0.18	0.03	0.14	0.37	0.00	Coating
CHI-12	100		0.708618			53.30	43.55	0.00	0.11	0.39	0.19	0.04	0.00	0.08	0.00	0.05	0.03	1.74	0.51	0.00	Stalact
CHI-14	100		0.708671			54.56	43.76	0.00	0.46	0.00	0.03	0.00	0.00	0.01	0.00	0.00	0.01	0.77	0.41	0.00	Globules
CHI-15	100																				Stalact

Fig. 2. Speleothems from Covón/Chifletera and their location on a schematic cross-section of the lava tube. a) Globules; b) crystalline crusts; c) crystal coatings; d) powder filling fractures; e) powder covering floor of lava tube and accumulating on ledges on walls; f) stalactites.

the white gypsum powder is covered by an orange dust mainly composed of quartz and phyllosilicates mixed with gypsum and halite.

On walls, powder accumulates in ledges forming layers up to 10 cm thick that cover areas from a few cm² up to a few dm² wide (Fig. 3a). On the floor, powder covers most of the surface and forms mounds of variable thickness, from just a few cm up to 60 cm (Fig. 3b). Sometimes, the surface of powder accumulations displays a white or orange crust usually <1 mm thick (Fig. 3b).

Powder is formed by a mass of randomly arranged crystals showing morphologies that vary from square platelets up to 100 μm size and 5 μm thick (Fig. 3c) to euhedral elongated bladed crystals 70 μm long, 15 μm wide and <5 μm in thickness. Most commonly, gypsum crystals appear either totally loose or weakly welded together. However, in some areas, they are cemented by halite (Fig. 3d–f). Gypsum powder can appear also inside fractures of the basalt host rock (Fig. 4a). These fractures are up to 3 cm wide. Powder can be present only in the most external part of the fracture (2–3 cm) (Fig. 4b, c), while in some cases

it fills the fracture up to at least 60 cm. Powder mounds are located on the floor just below fractures filled with powder (Fig. 4a).

5.1.2. Coatings

In some of the vacuoles and fractures of volcanic host rock, and sometimes on the walls, transparent acicular or bladed gypsum crystals grow perpendicularly to the surface, coating the cavities (Fig. 5a). The crystals are very delicate and easily detach from the wall by gravity. Their size is very uniform, between 1 and 5 μm thick, around 10 μm wide and up to 150 μm long (Fig. 5b). They are euhedral and show no signs of dissolution. Some coatings cover recently exposed surfaces like a bird skull or a small area on the lava tube floor where powder was recently washed away by dripping water.

5.1.3. Globules

Globules (Fig. 6) are botryoidal speleothems ranging in size from few mm to several cm, generally occurring on the lava tube ceiling.
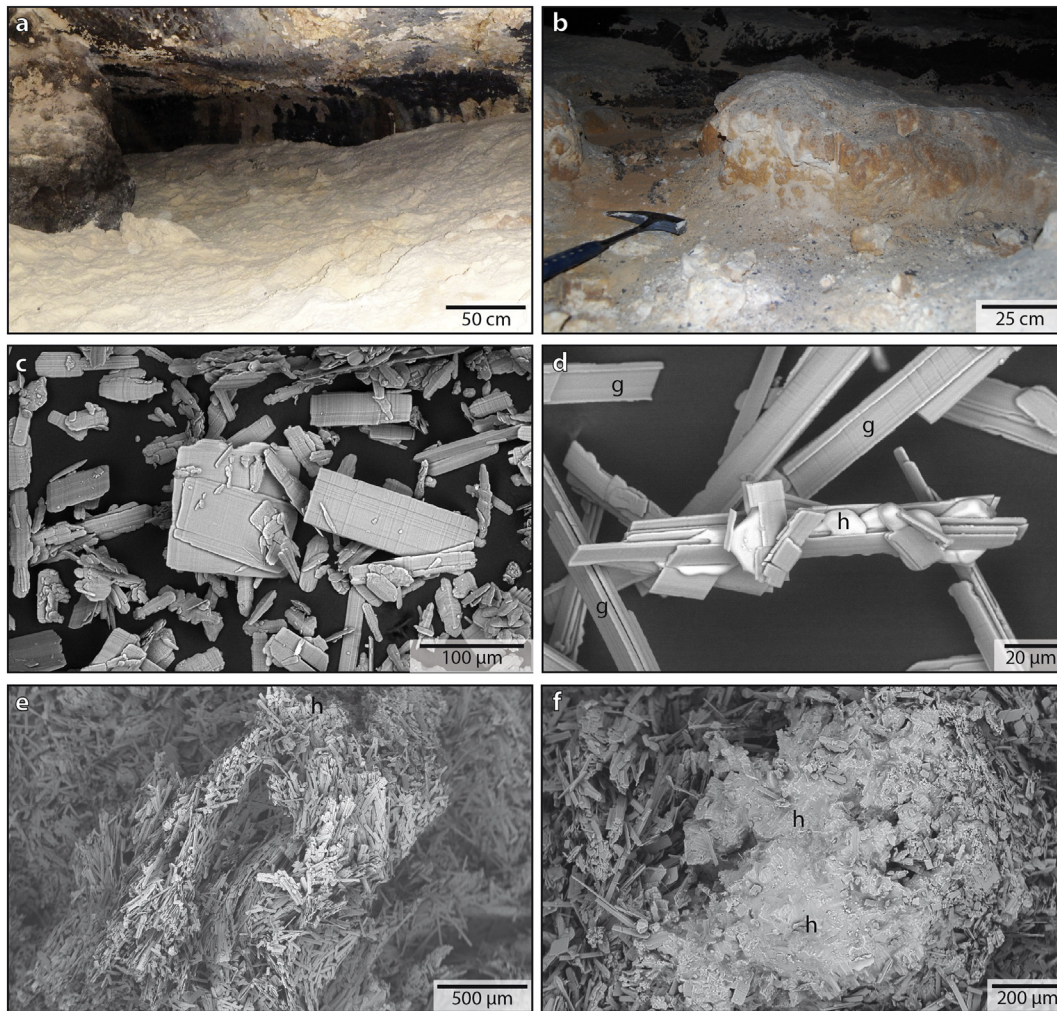
Fig. 3. Powder speleothems. a) Accumulation of powder on a ledge on the wall; b) mound of powder approximately 30 cm thick showing thin orange crusts over surface; c) SEM image of loose aggregates of gypsum crystals of heterogeneous size and shape, d) SEM image of elongated tabular gypsum crystals (g), some of them cemented by halite (h); e and f) SEM images of gypsum crystals cemented by halite (h) which form thin crusts over the powder accumulations.
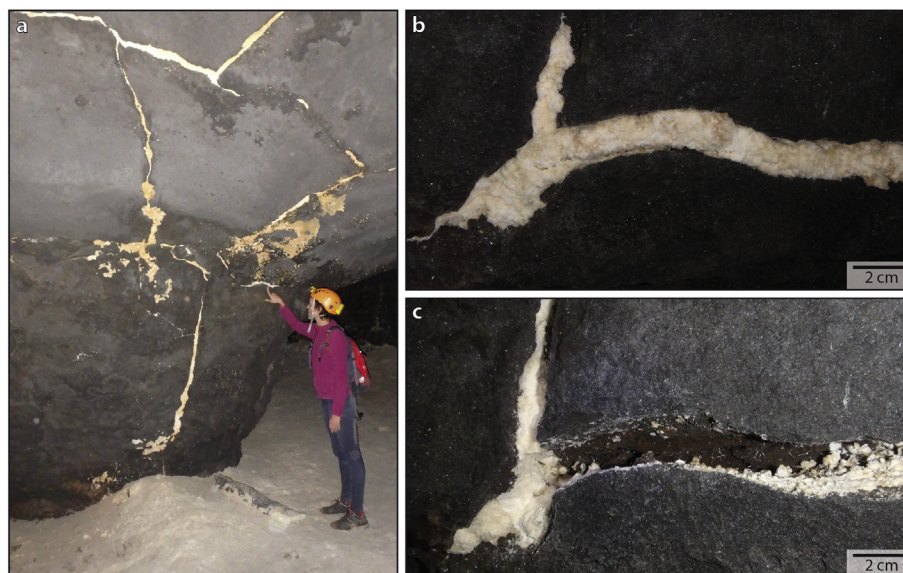
Fig. 4. Fractures filled by powder speleothems. a) General view of the lava tube showing associated crystalline crusts and a mound of powder at tube floor below a fracture. b) Fracture completely filled by powder. c) Fracture partially filled by powder and crystal coatings inside.
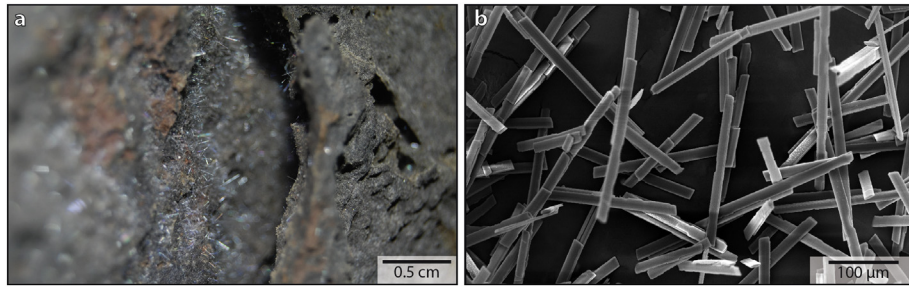
Fig. 5. Crystal coatings. a) Transparent acicular gypsum crystals growing perpendicular to substrate on a vacuole of host rock; b) SEM image of euhedral acicular crystals.

They are formed by white microcrystalline aggregates that are either crumbly or compact. Some globules are white (Fig. 6c) whereas others have an external indurated orange crust (Fig. 6a and b).

In thin section, globules have the following textures: a) an external orange crust composed of lenticular crystals 0.4 mm long, arranged perpendicularly to the outer surface (Fig. 6d); b) internal crumbly aggregates composed of lenticular crystals 120 μm long and 40 μm wide contained in a mass of smaller fibrous crystals 50 to 70 μm (Fig. 6e); c) internal compact aggregates composed of randomly arranged masses of homogeneous fibrous crystals up to 120 μm (Fig. 6f).

5.2. Macrocrystalline gypsum

It constitutes compact speleothems composed of tabular or lenticular crystals reaching millimetric sizes. They can be classified as follows.

5.2.1. Crusts

Crusts (Fig. 7a–c) are compact beige, orange or yellow deposits, which appear mostly on the upper part of walls and ceilings of the lava tubes. They are up to 5 mm thick and occur scattered as patches that cover areas of some dm2 (Fig. 7b). Crusts are composed of tabular or lenticular crystals, sometimes forming rosettes (Fig. 7c), and apparently they are not connected with any visible fracture or crack in the host rock. In thin section gypsum crystals show various morphologies, but they are usually elongated and form fans that cross each other in all directions. Their size ranges from 0.2 to 5 mm long and up to 1 mm wide (Fig. 7g and h).

5.2.2. Stalactites

Stalactites are relatively common in both lava tubes and appear along the whole tube without any particular distribution. They are orange and translucent and occur in groups on ceilings, protruding out of gypsum crusts (Fig. 7d). Gypsum stalactites are conical, up to 4 cm long and about 1–2 cm wide (Fig. 7e) and composed of lenticular and tabular crystals forming fans and rosettes, which results in an irregular outer texture. They lack an internal channel and at the moment of sampling were totally dry, we have not observed dripping on any of them. In thin section they show the same characteristics as crusts (Fig. 7g and h).

Between some crusts and the basaltic host-rock a botryoidal layer, less than 1 mm thick (Fig. 8), has been observed. Under the microscope it is reddish-brown with laminar or irregular shapes (Fig. 8a). Crystal morphology and EDS analyses performed in SEM (Si O and small amounts of Fe) (Fig. 8b–d) suggest that it is composed of opal.

5.2.3. Laminated crusts

Laminated crusts are up to 10 cm thick accumulations of compact gypsum observed only in Covón lava tube. They appear in the lower
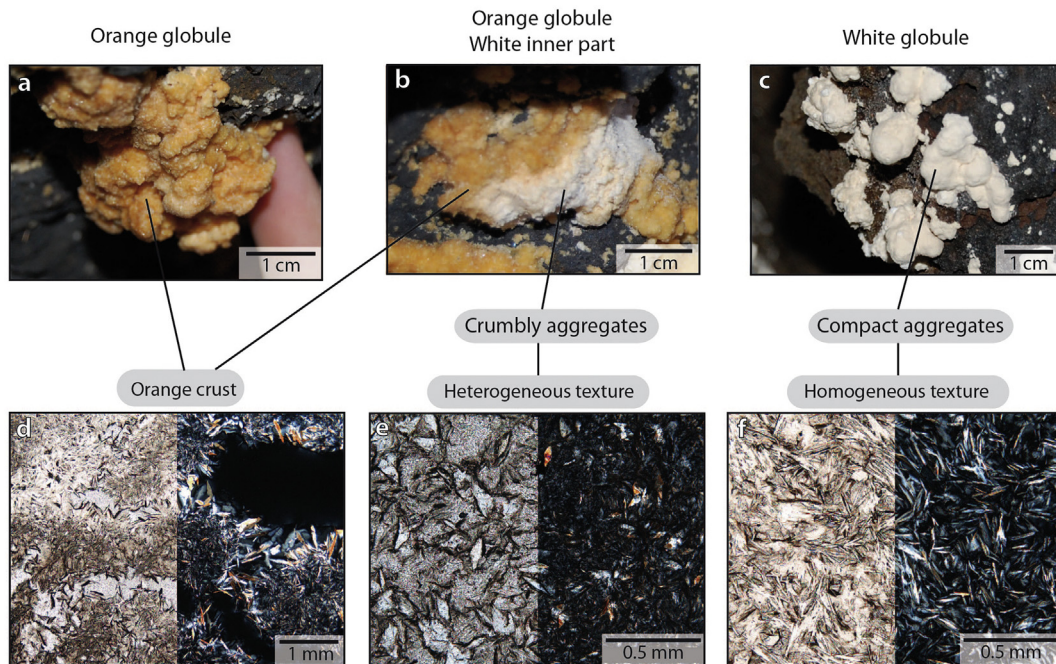
Fig. 6. Globular speleothems. a) Unaltered globule showing an external orange crust; b) broken globule showing an inner white part with crumbly texture; c) unaltered white globule showing compact texture; d) microphotograph (left, plane polarised light and right, cross polarised light) of the orange crust (a), formed by lenticular crystals of about 0.4 mm arranged perpendicular to outer surface; e) microphotograph of crumbly aggregates showing two types of crystals: lentils of about 120 μm floating in a mass of much smaller (50 μm) acicular crystals; f) microphotograph of compact aggregates, composed of fibrous, homogeneous in size, crystals.
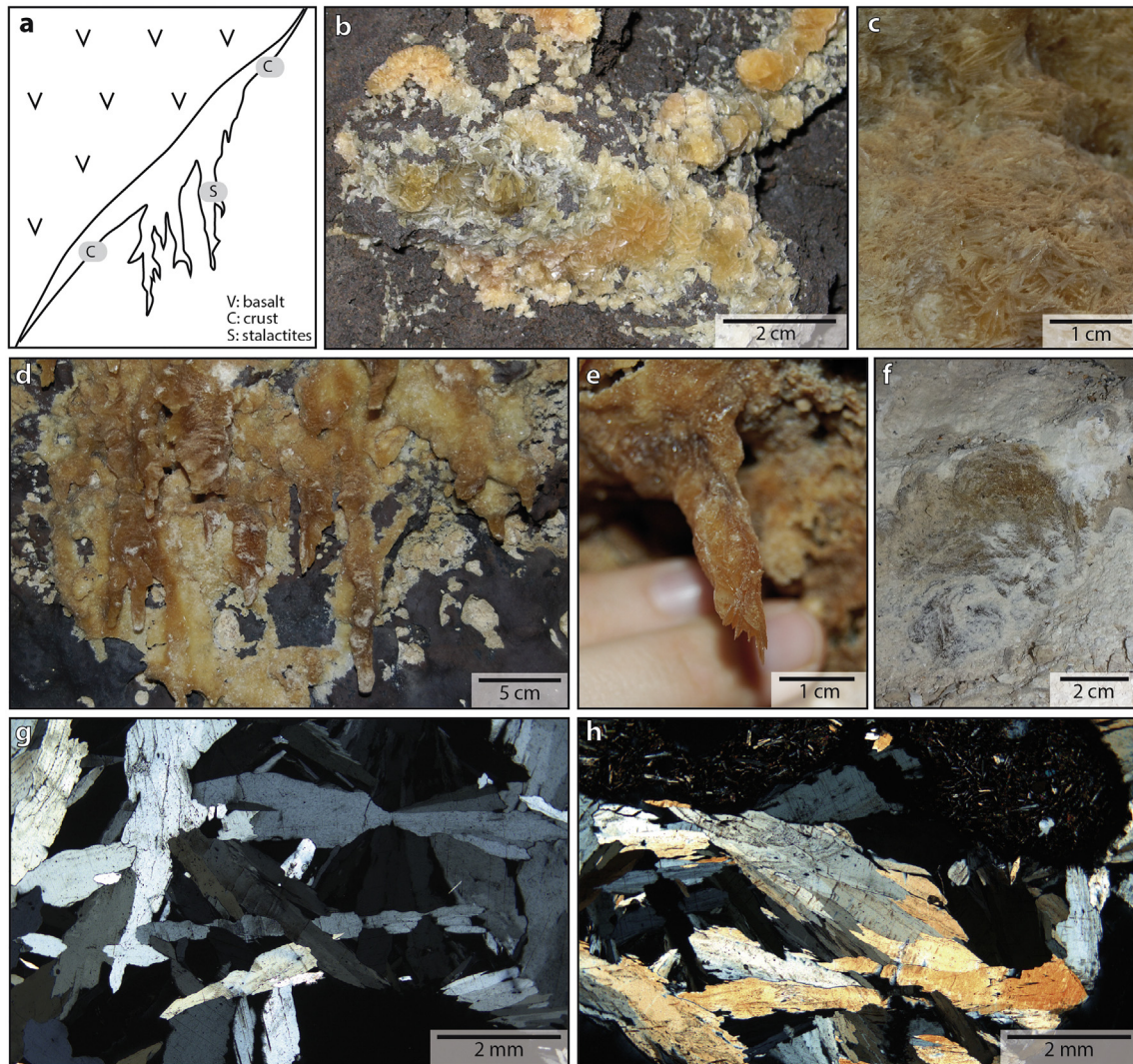
Fig. 7. Macrocrystalline speleothems. a) Sketch showing different parts of crystalline speleothems; b and c) crusts composed of lenticular crystals arranged in roses; d) gypsum stalactites developing from crusts; e) detail of tip of a stalactite; f) laminated crust developed on powder accumulations and below stalactites and crusts; g and h) microphotographs of crusts and stalactites under cross polarised light. Elongated and lenticular gypsum crystals of up to 4 mm long form fans that cross each other in all directions.

part of walls, over powder accumulations and below areas of the ceiling that have crusts or stalactites (Fig. 7f). This speleothem is similar to ceiling crusts, but in some areas has a faint internal lamination. They are often weathered, broken and/or covered with gypsum powder.

6. Geochemistry

6.1. X-ray fluorescence

XRF shows no differences in any element content among samples with different textures. Results reported below refer to all analysed samples excluding CHI-6, which is very different due to its higher Na and Cl content. All analyses display higher Ca than S contents.

Covón samples show the highest contents in Cl, Mg, Al, Ti and Fe. Speleothems of both lava tubes have similar Sr, Si, and K contents. Br appears sporadically and in very small amounts (Table 1).

Some pairs of elements display linear trends (Fig. 9), with high r^2 values, mainly in Covón. This is the case of the relationships between Si-Al, Fe-Al, and Fe-Si ($r^2 > 0.9$). Ca-S, Si-Mg and Al-Mg relationships show r^2 values between 0.5 and 0.9. In Chifletera linear trends between elements have lower r^2 values than in Covón, being the highest, Fe-Al ($r^2 = 0.86$), Si-Al ($r^2 = 0.66$) and Fe-Si ($r^2 = 0.62$). However, the existence of outliers in such relationships (Fig. 9) together with the small amount of data, do not allow to consider any of them as correlated.

6.2. $^{87}Sr/^{86}Sr$

The $^{87}Sr/^{86}Sr$ ratios for our gypsum speleothems range between 0.708665 and 0.708976 (Table 1). The lowest values correspond to Chifletera, showing a difference of 0.0005 with respect to the present day marine value (0.7092), whereas those from Covón differ only by 0.0003 (Fig. 10). Obtained values are similar to those of the calcretes from Lanzarote and Fuerteventura developed on aeolian sandstones with marine bioclasts. These are the main source of marine-derived Ca (Huerta et al., 2015).

6.3. Stable isotopes and uranium series dating

Stable isotopic values of gypsum speleothems range from 20.7 to 21.7‰ (mean value of 20.97‰) V-CDT for $\delta^{34}S$, and from 9.12 to 10.43‰ (mean value of 9.78‰) V-SMOW for $\delta^{18}O$ (Fig. 11).

Analysed samples (Table 2) show ages that range from 40,039 ± 4748 yr to 6217 ± 1644 yr. Accordingly, gypsum from Covón, (PAR) and Chifletera (CHI) precipitated from the Upper Pleistocene to Holocene, during Marine Isotope Stages (MIS) 3 to 1.
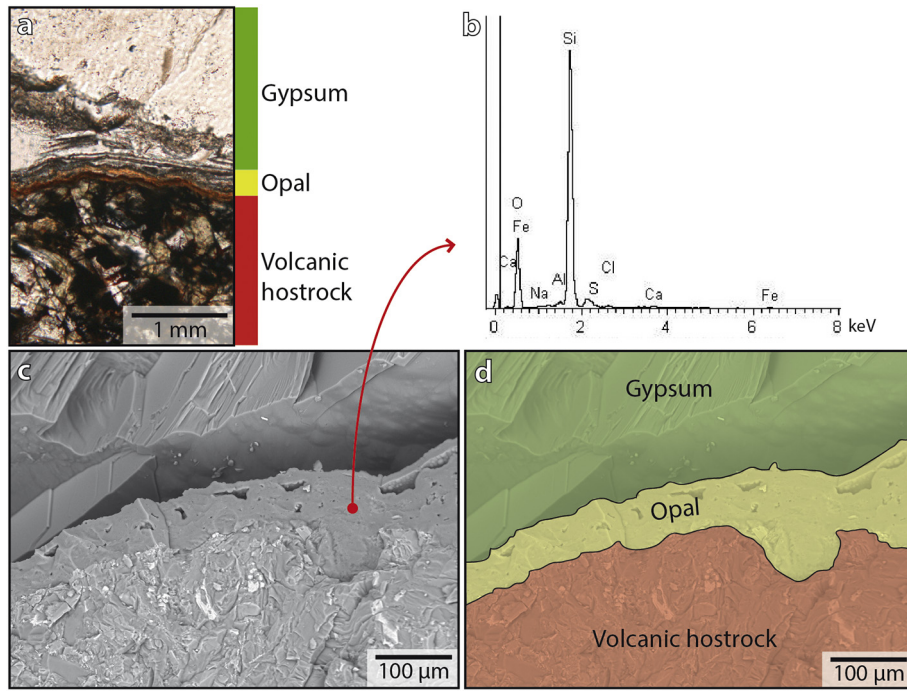
Fig. 8. Botryoidal layer between some crusts and basaltic host-rock. a) Microphotograph under plane polarised light (left) and petrographic identification (right); b) EDS analysis performed under SEM. c) SEM image of botryoidal layer, and d) color map over SEM image, separating the different parts.

7. Discussion

7.1. SO_4^{2-} and Ca supply

Geochemical and isotopic analyses indicate that the origin of the sulphate and Ca forming the gypsum speleothems from Covón and Chifletera is seawater.

The $^{87}Sr/^{86}Sr$ values for gypsum are close to those of seawater (0.7092; see Whipkey et al., 2000), and thus the main source of Ca (Sr) should also be seawater. Slight differences between gypsum and seawater values are interpreted as indicating a secondary source of Sr, such as aeolian dust or volcanic rocks. However, the low content in Ti, Mn and Ni, and the low r^2 values of the linear trends Si-Mg; Si-Fe; Si-Ca (typical elements in basalt minerals like olivine and plagioclase) observed in XRF and the major differences with Sr ratios from Lanzarote basalts (0.703317) indicate that the volcanic rock contribution is minor. The higher Ca content with respect to S, together the low r^2 values between both elements suggest an additional mineral phase containing Ca supporting the idea of aeolian dust contribution in these lava tubes (Fig. 9). The contribution of aeolian dust coming from Sahara Desert and Sahel has been recognized in travertines from Gran Canaria (Rodríguez-Berriguete et al., 2018) and in Lanzarote calcretes (Huerta et al., 2015), but the latter show wider ranges of $^{87}Sr/^{86}Sr$ than those of the gypsum from lava tubes. Probably this is a consequence of the variety of rocks (in composition and age) from which the aeolian dust is derived (Menéndez et al., 2007; Hefferan et al., 2014). However, calcretes developed on aeolian sands composed of marine bioclasts have Sr ratios similar to seawater (Fig. 10).

$\delta^{34}S$ and $\delta^{18}O$ values of gypsum from lava tubes of Lanzarote reflect those of the sulphate dissolved in modern seawater. Gypsum precipitated from seawater usually displays the same values than dissolved sulphate ($\delta^{34}S$ of 20–21‰ V-CDT, and $\delta^{18}O$ of about 9.5–9.6‰ V-SMOW) (Hoefs, 2008), or the gypsum isotopes are slightly enriched compared to those of dissolved sulphate by 1.65–1.7 and 3.5–3.6‰, in $\delta^{34}S$ and $\delta^{18}O$, respectively (Mayer, 2005; Warren, 2006). Differences between $\delta^{34}S$ and $\delta^{18}O$ values of marine dissolved sulphate and gypsum speleothems are lower than those reported by Warren (2006) and

Mayer (2005) in marine evaporites, so fractionation and/or mixing processes for both isotopes are minor (Fig. 11).

7.2. Age of speleothems

Speleothems show a wide range of ages, from Upper Pleistocene to Holocene, and formed in warm and cold marine isotope stages. The wide range of the ages measured (Table 2), the different climatic conditions in which speleothems formed and the occurrence of crystal coatings developed on recent surfaces suggest that speleothems are still forming during the present day.

7.3. Solution pathways

Isotopic data show that seawater is the main source of ions for the formation of speleothems. Seawater can reach the lava tubes in a variety of ways (Fig. 12).

7.3.1. Pathway 1

Marine spray entering the lava tube is composed of micrometric seawater drops (Taylor and Wu, 1992), which can partially evaporate inside the cave, increasing their solute concentration and thus precipitating gypsum. During air circulation, micro drops evaporate only partially due to the high relative humidity in the coastal areas of Lanzarote (60–70%). Evaporation concentrates micro drops allowing gypsum precipitation, but halite oversaturation is rarely reached, as occurs in areas with relative humidity higher than 80% (Sonnenfeld, 1984). Sea spray is considered a common source of ions for formation of evaporative minerals in caves near the coast (Bottrell et al., 1993; Onac et al., 2009).

7.3.2. Pathway 2

Marine spray in the exterior of the cave causes precipitation of salts that are later dissolved during rain events, and transported inside the lava tubes. Here they affected by evaporation, thus becoming oversaturated with respect to gypsum. In Fuerteventura, airborne salts
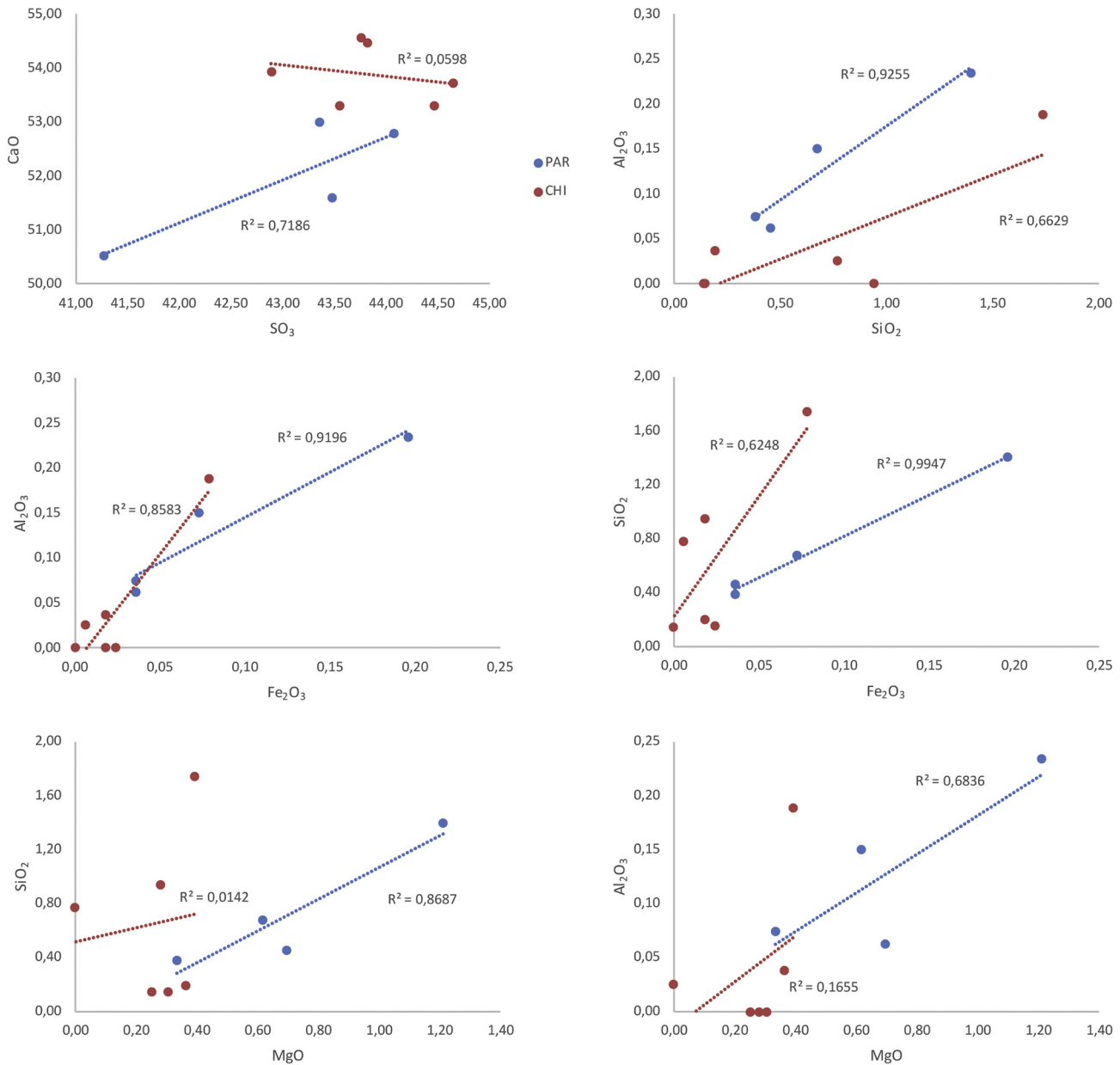
Fig. 9. Comparison between different element (expressed as oxides) obtained through XRF for Covón (blue rhombs) and Chifletera (red squares) lava tubes. All data are referred in mol (%).

from sea spray are carried by rainfall into groundwaters, increasing their salinity (Custodio, 1990; Herrera and Custodio, 2000).

7.4. Mechanisms of speleothems formation

Direct evaporation is the main process to concentrate the brine, and later oversaturate it with respect to gypsum. Morphological variations and textures of gypsum speleothems are influenced by the amount and pathway of water (infiltrated water vs. sea spray aerosols), the type of water flow (capillarity, drip), the temperature of the rock and the air, the relative humidity and the presence of air currents in the lava tube.

Microcrystalline gypsum crystals, such as those composing coatings and powder, are known to precipitate in conditions of high supersaturation usually caused by fast evaporation (Forti, 2017). The presence of an airflow can enhance evaporation (Calaforra and Forti, 1994; Buecher, 1999; Gázquez et al., 2011), of marine spray entering the tube, triggering precipitation of very small bladed or fibrous crystals. The droplets

forming marine spray can deposit through several mechanisms, as for instance, interception or impaction with an obstacle and sedimentation, depositing by gravity when the airflow can no longer transport them (Dredge et al., 2013). When droplets impact the surface of the basalt on the tube walls, they evaporate and form coatings, when they deposit by gravity, powder forms on the floor. The presence of coatings on recently exposed surfaces indicates that some of these crystals are precipitating today, and this process is still taking place.

Powder accumulations probably result from the repetition through time of the previously described processes, when sea spray entering the cave evaporates precipitating microcrystalline gypsum directly in the air or on walls as coatings, which later falls and accumulates on the floor and wall ledges.

Similar accumulations, also called gypsum powder or gypsum snow, have been interpreted as disintegration of other fibrous speleothems (Hill and Forti, 1997), weathering products of crusts (James, 1991) or evaporation of capillary waters (Calaforra and Forti, 1994; Hill and Forti, 1997).
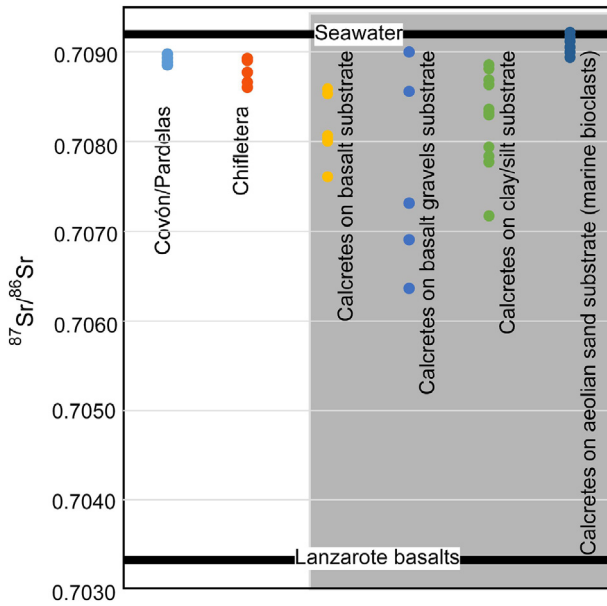
Fig. 10. $^{87}Sr/^{86}Sr$ ratios for speleothems from Covón and Chifletera lava tubes. Present-day seawater, Lanzarote basalts and calcretes developed on different substrates (Huerta et al., 2015) are plotted (grey area).

Gypsum powder filling fractures can form by direct precipitation from sea spray entering tubes and fractures. Alternatively, powder filling cracks could have precipitated from water coming from above, from outside the tube (Pathway 2). Rainwater would dissolve sea salts from the surface and enter the fractures. If the amount of water is small enough to form a capillary film highly supersaturated in gypsum, small bladed and platy crystals typical of gypsum powder can precipitate in the cracks (Fig. 4).

Macrocrystalline gypsum crystals, such as the ones forming crusts and stalactites, require low levels of supersaturation (Forti, 2017) and

hence, reduced nucleation rates (Otalora and Garcia-Ruiz, 2014). Such situations could be possibly due to: 1) direct precipitation in periods of rainfall when infiltrated water would dissolve airborne salts deposited outside the cave, reaching only smaller values of supersaturation when arriving inside the lava tube; 2) process of dissolution of microcrystalline gypsum and slow reprecipitation of larger crystals in the following two contexts: A) in stages of high rainfall, by infiltration of meteoric water undersaturated with respect to gypsum. B) Dissolution can be caused by condensation of water on the speleothems if humid air warmer than the speleothems surface enters the lava tube. Dissolution and reprecipitation of microcrystalline gypsum on the outer surface of globules can explain the presence of the outer crust composed of larger crystals, while the internal part of globules remains microcrystalline (Fig. 6a, b). Condensation water dissolving gypsum powder and slowly dripping along the wall, while slowly evaporating, would produce crusts and stalactites not connected to major fractures or cracks. Condensation is a relatively common phenomenon in caves, including those developed in semiarid climates (Gázquez et al., 2015), where recent stable isotope studies have highlighted its role in precipitation of gypsum speleothems (Gázquez et al., 2017).

Laminated crusts probably have also formed by processes of dissolution and re-precipitation of powder accumulations caused by water dripping, as suggested by their location below groups of stalactites. Lamination would form by alternation of dripping processes with gypsum dust deposition, similarly as it has been described in Cueva del León, Argentina, where so-called "gypsum dust flowstones" form by alternation of dry periods with very short wet periods, when dripping water partially dissolves and further cements gypsum powder, forming layers (Hill and Forti, 1997; Forti, 2017).

8. Conclusions

El Covón-Chifletera lava tubes located in Lanzarote (Canary Islands) contains microcrystalline gypsum speleothems such as: 1) powder accumulations, 2) coatings, 3) globules; and macro-crystalline speleothems such as: 4) crusts, 5) stalactites and 6) laminated crusts.
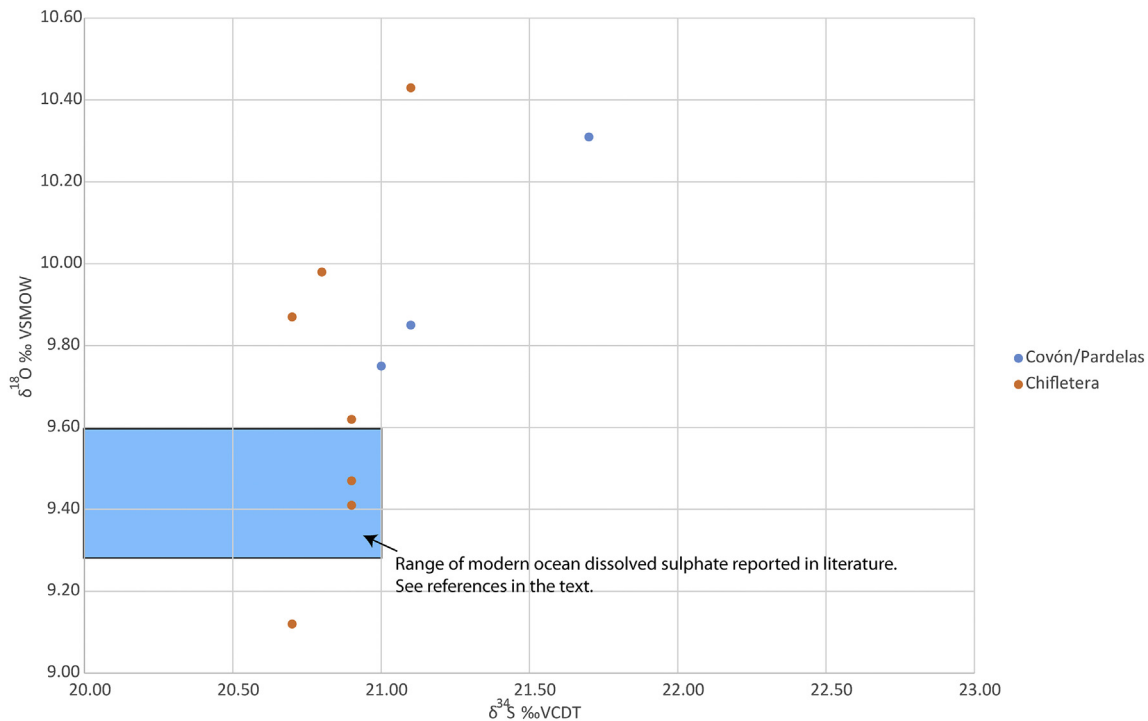

Fig. 11. $\delta^{34}S$ vs $\delta^{18}O$ plot of speleothems from Covón and Chifletera lava tubes. For more details see Table 1.

Table 2
Uranium series dating of gypsum speleothems from Covón and Chifletera lava tubes. All errors are absolute 2σ values. Subsample powder sizes range from 70 to 130 mg. Initial ^{230}Th/^{232}Th atomic ratio used to correct ages is 0.0000044 (activity ratio = 0.8) ± 50%. Years BP = years before present, where present = AD 2018.

Sample	^{238}U (ng/g)	^{232}Th (pg/g)	^{230}Th/^{232}Th	^{230}Th/^{238}U	δ^{234}U$_{measured}$	δ^{234}U$_{initial}$	Uncorrected age (years BP)	Corrected age (years BP)	Speleothem (type)
CHI-15	129.8 ± 0.1	14,767 ± 32	2.29 ± 0.05	0.085 ± 0.002	21 ± 2	22 ± 2	9506 ± 203	6217 ± 1644	Stalactite
CHI-16	33.3 ± 0.1	13,446 ± 59	2.30 ± 0.03	0.304 ± 0.004	96 ± 4	103 ± 4	35,197 ± 520	24,017 ± 5472	Powder
CHI-18	68.8 ± 0.1	23,351 ± 79	3.51 ± 0.03	0.390 ± 0.004	62 ± 3	69 ± 4	49,676 ± 609	40,039 ± 4748	Powder
PAR-11	110.7 ± 0.3	26,342 ± 88	3.52 ± 0.03	0.274 ± 0.002	85 ± 6	92 ± 6	31,586 ± 389	25,055 ± 3237	Stalactite
PAR-12	69.7 ± 0.1	13,309 ± 22	2.83 ± 0.03	0.176 ± 0.002	81 ± 3	84 ± 3	19,399 ± 261	14,154 ± 2603	Crust
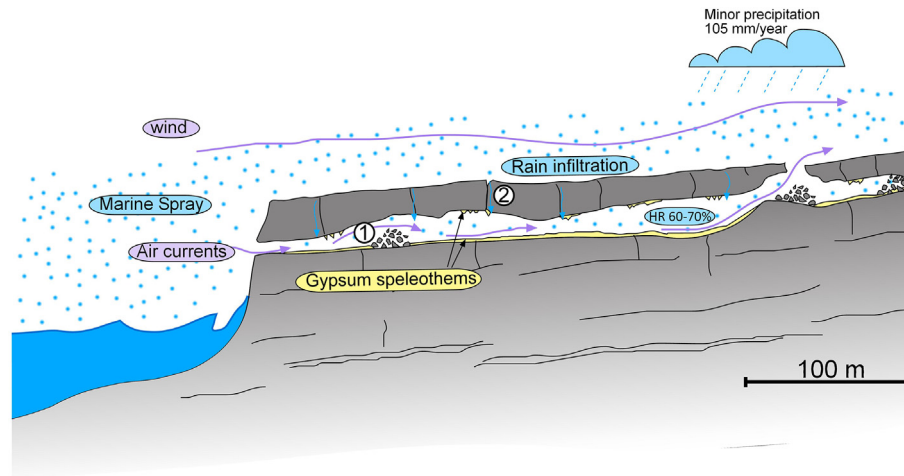
Fig. 12. Sketch showing different processes and pathways for ion input involved in the origin of gypsum speleothems. 1) Marine spray entering the lava tube; 2) airborne salts from surface are dissolved during rain event and infiltrated into the lava tube.

Gypsum speleothems, formed over the past 40,039 ± 4748 yr BP to 6217 ± 1644 yr BP (Upper Pleistocene-Holocene), and the process is still active. They formed probably under dominant evaporating conditions interrupted by episodic rainy periods.

Sea spray is the main source of ions in the formation of gypsum speleothems in lava tubes of Lanzarote as indicated by the δ^{34}S, δ^{18}O, and ^{87}Sr/^{86}Sr ratios of gypsum. Two pathways for ion input in the lava tube have been considered. 1) Sea spray circulating within the lava tube; 2) salt precipitation above the lava tube, followed by dissolution by scant rains and percolation underground.

Microcrystalline gypsum formed under high supersaturation conditions produced by the fast evaporation of marine spray due to the small size of spray particles. On the other hand, macrocrystalline gypsum speleothems formed under low supersaturation conditions favoured by infiltration of rainwaters that dissolved salts on the surface, and/or by dissolution-reprecipitation produced by undersaturated infiltration waters or by condensation processes on microcrystalline gypsum.

Large accumulations of gypsum are possible when precipitation is scarce because in rainy climates gypsum deposits are dissolved by rainfall. The constant input of sea spray into the cave, the presence of air currents and the partial but rapid evaporation of sea spray produce large amounts of gypsum precipitation.

References

Alonso-Zarza, A.M., Silva, P.G., 2002. Quaternary laminar calcretes with bee nests: evidences of small-scale climatic fluctuations, Eastern Canary Islands, Spain. Palaeogeography Palaeoclimatology Palaeoecology 178 (1–2), 119–135.

Alonso-Zarza, A.M., Bustamante, L., Huerta, P., Rodríguez-Berriguete, Á., Huertas, M.J., 2016. Chabazite and dolomite formation in a dolocrete profile: an example of a complex alkaline paragenesis in Lanzarote, Canary Islands. Sedimentary Geology 337, 1–11.

Asmerom, Y., Polyak, V.J., Burns, S.J., 2010. Variable winter moisture in the southwestern United States linked to rapid glacial climate shifts. Nature Geoscience 3, 114.

Bottrell, S.H., Carew, J.L., Mylroie, J.E., 1993. Inorganic and bacteriogenic origin for sulfate crusts in flank margin cave, San Salvador Island, Bahamas. In: White, B. (Ed.), Proc. of the 6th Symposium on the Geology of the Bahamas. Bahamian Field Station, San Salvador, pp. 17–21.

Buecher, R.H., 1999. Microclimate study of Kartchner caverns, Arizona. Journal of Cave and Karst Studies 61 (2), 108–120.

Calaforra, J.M., Forti, P., 1994. Two new types of gypsum speleothems from New Mexico: gypsum trays and gypsum dust. National Speleological Society Bulletin 56, 32–37.

Calaforra, J., Forti, P., Fernandez-Cortes, A., 2008. Speleothems in gypsum caves and their paleoclimatological significance. Environmental Geology 53 (5), 1099–1105.

Carracedo, J.C., Rodriguez Badiola, E., Soler, V., 1992. The 1730–1736 eruption of Lanzarote, Canary Islands: a long, high-magnitude basaltic fissure eruption. Journal of Volcanology and Geothermal Research 53 (1–4), 239–250.

Carracedo, J.C., Singer, B., Jicha, B., Guillou, H., Rodríguez Badiola, E., Meco, J., Pérez Torrado, F.J., Gimeno, D., Socorro, S., Láinez, A., 2003. The eruption and lava tubes of Corona Volcano (Lanzarote, Canary Islands). Estudios Geológicos 59 (5–6), 277–302.

Coudé-Gaussen, G., Rognon, P., Bergametti, G., Gomes, L., Strauss, B., Gros, J.M., Le Coustumer, M.N., 1987. Saharan dust on Fuerteventura Island (Canaries): chemical and mineralogical characteristics, air mass trajectories, and probable sources. Journal of Geophysical Research 92 (D8), 9753–9771.

Criado, C., Torres, J.M., Hansen, A., Lillo, P., Naranjo, A., 2012. Intercalaciones de polvo sahariano en paleodunas bioclásticas de Fuerteventura (Islas Canarias). Cuaternario y Geomorfología 26 (1–2), 73–88.

Criado, C., Dorta, P., Bethencourt, J., Navarro, J.F., Romero, C., García, C., 2013. Evidence of historic infilling of valleys in Lanzarote after the Timanfaya eruption (AD 1730–1736, Canary Islands, Spain). Holocene 23 (12), 1786–1796.

Custodio, E., 1990. Saline groundwater in the Canary Islands (Spain) resulting from aridity. In: Paepe, R., Fairbridge, R.W., Jelgersma, S. (Eds.), Greenhouse Effect, Sea Level and Drought. Springer Netherlands, Dordrecht, pp. 593–618.

Dillon, J.R., Polyak, V.J., Asmerom, Y., 2009. Dating of Quaternary eruption events using U-series ages of lava cave gypsum crusts. Geological Society of America Annual meeting. Abstracts with Programs v. 41. 7. Geological Society of America, Portland, p. 193.

Dredge, J., Fairchild, I.J., Harrison, R.M., Fernandez-Cortes, A., Sanchez-Moral, S., Jurado, V., Gunn, J., Smith, A., Spötl, C., Mattey, D., Wynn, P.M., Grassineau, N., 2013. Cave aerosols: distribution and contribution to speleothem geochemistry. Quaternary Science Reviews 63 (0), 23–41.

Forti, P., 2005. Genetic processes of cave minerals in volcanic environments: an overview. Journal of Cave and Karst Studies 67 (1), 3–13.

Forti, P., 2017. Chemical deposits in evaporite caves: an overview. International Journal of Speleology 46 (2), 109–135.

Galdenzi, S., Menichetti, M., 1995. Occurrence of hypogenic caves in a karst region: examples from central Italy. Environmental Geology 26 (1), 39–47.

Gázquez, F., Calaforra, J.-M., Sanna, L., Forti, P., 2011. Espeleotemas de yeso:¿ Un nuevo proxy paleoclimático. Boletín de la Real Sociedad Española de Historia Natural. Sección Geología 105 (1–4), 15–24.

Gázquez, F., Calaforra, J.-M., Forti, P., De Waele, J., Sanna, L., 2015. The role of condensation in the evolution of dissolutional forms in gypsum caves: study case in the karst of Sorbas (SE Spain). Geomorphology 229, 100–111.

Gázquez, F., Calaforra, J.M., Evans, N.P., Hodell, D.A., 2017. Using stable isotopes (δ^{17}O, δ^{18}O and δD) of gypsum hydration water to ascertain the role of water condensation in the formation of subaerial gypsum speleothems. Chemical Geology 452, 34–46.

Gómez-Ortiz, D., Montesinos, F.G., Martín-Crespo, T., Solla, M., Arnoso, J., Vélez, E., 2014. Combination of geophysical prospecting techniques into areas of high protection value: identification of shallow volcanic structures. Journal of Applied Geophysics 109, 15–26.

Hefferan, K., Soulaimani, A., Samson, S.D., Admou, H., Inglis, J., Saquaque, A., Latifa, C., Heywood, N., 2014. A reconsideration of Pan African orogenic cycle in the Anti-Atlas Mountains, Morocco. Journal of African Earth Sciences 98, 34–46.

Herrera, C., Custodio, E., 2000. Saline Water in Central Fuerteventura Island, Canary Islands, Spain, 16th Salt Water Intrusion Meeting. Miedzyzdroje–Wollin Island, Poland, pp. 81–86.

Hill, C.A., Forti, P., 1997. Cave Minerals of the World. National Speleological Society, Huntsville, AL (463 pp.).

Hoefs, J., 2008. Stable Isotope Geochemistry. Springer Science & Business Media.

Huerta, P., Rodríguez-Berriguete, Á., Martín-García, R., Martín-Pérez, A., La Iglesia Fernández, Á., Alonso-Zarza, A.M., 2015. The role of climate and aeolian dust input in calcrete formation in volcanic islands (Lanzarote and Fuerteventura, Spain). Palaeogeography, Palaeoclimatology, Palaeoecology 417 (0), 66–79.

Jakobsson, S.P., Jónsson, S.S., Leonardsen, E., 1992. Encrustations from lava caves in Surtsey, Iceland. A Preliminary Report, Surtsey Research Progress Report, pp. 73–78.

James, J.M., 1991. The sulfate speleothems of Thampanna Cave, Nullarbor Plain, Australia. Helictite 29, 19–23.

LaPointe, Z., Polyak, V., Asmerom, Y., 2013. Uranium and strontium isotope study of late-stage speleothems from lava tube caves in El Malpais National Monument, New Mexico. In: Zeigler, K., Timmons, J.M., Timmons, S., Semken, S. (Eds.), Geology of Route 66 Region: Flagstaff to Grants. New Mexico Geological Society 64th Annual Fall Field Conference Guidebook. New Mexico Geological Society, New Mexico, pp. 223–228.

Lipar, M., Ferk, M., Lojen, S., Barham, M., 2019. Sulfur (^{34}S/^{32}S) isotope composition of gypsum and implications for deep cave formation on the Nullarbor Plain, Australia. International Journal of Speleology 48 (1) (in press).

Mayer, B., 2005. Assessing Sources and Transformations of Sulphate and Nitrate in the Hydrosphere Using Isotope Techniques, Isotopes in the Water Cycle. Springer, pp. 67–89.

Menéndez, I., Díaz-Hernández, J.L., Mangas, J., Alonso, I., Sánchez-Soto, P.J., 2007. Airborne dust accumulation and soil development in the North-East sector of Gran Canaria (Canary Islands, Spain). Journal of Arid Environments 71 (1), 57–81.

Onac, B.P., 2012. Minerals. In: White, W.B., Culver, D.C. (Eds.), Encyclopedia of Caves, Second edition Academic Press, Amsterdam, pp. 499–508.

Onac, B.P., Forti, P., 2011. Minerogenetic mechanisms occurring in the cave environment: an overview. International Journal of Speleology 40 (2), 79–98.

Onac, B.P., Sumrall, J., Mylroie, J.E., Kearns, J.B., 2009. Cave Minerals of San Salvador Island, Bahamas. Karst Studies Series 1. University of South Florida Tampa Library (70 pp.).

Otalora, F., Garcia-Ruiz, J., 2014. Nucleation and growth of the Naica giant gypsum crystals. Chemical Society Reviews 43 (7), 2013–2026.

Palmer, A.N., 6.20 Sulfuric Acid Caves: Morphology and Evolution. In: F.S. Editor-in-Chief: John (Ed.), Treatise on Geomorphology. (2013) Academic Press, San Diego, pp. 241–257.

Polyak, V.J., Provencio, P., 2001. By-product materials related to H_2S-H_2SO_4 influenced speleogenesis of Carlsbad, Lechuguilla, and other caves of the Guadalupe mountains, New Mexico. Journal of Cave and Karst Studies 63 (1), 23–32.

Prospero, J.M., Lamb, P.J., 2003. African droughts and dust transport to the Caribbean: climate change implications. Science 302 (5647), 1024–1027.

Rodríguez-Berriguete, Á., Alonso-Zarza, A.M., Martín-García, R., Cabrera, M.C., 2018. Sedimentology and geochemistry of a human-induced tufa deposit: implications for palaeoclimatic research. Sedimentology 65 (7), 2253–2277.

Sauro, F., Tisato, N., De Waele, J., Bernasconi, S.M., Bontognali, T.R.R., Galli, E., 2014. Source and genesis of sulphate and phosphate–sulphate minerals in a quartz-sandstone cave environment. Sedimentology 61 (5), 1433–1451.

Serantes Vergara, D., Pena Muiño, C., 2013a. Cueva del Covón o de la Chifletera. Tubos lávicos de Lanzarote. https://issuu.com/diegoserantesvergara7/docs/cueva_del_cov_n (pp. 17).

Serantes Vergara, D., Pena Muiño, C., 2013b. La Cueva del Esqueleto y sus hallazgos aborígenes. https://issuu.com/diegoserantesvergara7/docs/cueva_del_esqueleto (12 pp.).

Smith, G., 2015. Caves of Lanzarote. Guide to the caves with GPS co-ordinates. http://www.cavesoflanzarote.co.uk/documents/Cavesof%20Lanzarote%202%20medium.pdf (12 pp.).

Sonnenfeld, P., 1984. Brines and Evaporites. Academic Press (613 pp.).

Taylor, N.J., Wu, J., 1992. Simultaneous measurements of spray and sea salt. Journal of Geophysical Research: Oceans 97 (C5), 7355–7360.

Warren, J.K., 2006. Evaporites: Sediments, Resources and Hydrocarbons. Springer Science & Business Media.

Whipkey, C., Capo, R., Chadwick, O., Stewart, B., 2000. The importance of sea spray to the cation budget of a coastal Hawaiian soil: a strontium isotope approach. Chemical Geology 168 (1), 37–48.

White, W.B., 2010. Secondary minerals in volcanic caves: data from Hawai'i. Journal of Cave and Karst Studies 72 (2), 75–85.

Zazo, C., Goy, J.L., Hillaire-Marcel, C., Gillot, P.Y., Soler, V., González, J.A., Dabrio, C.J., Ghaleb, B., 2002. Raised marine sequences of Lanzarote and Fuerteventura revisited - a reappraisal of relative sea-level changes and vertical movements in the eastern Canary Islands during the Quaternary. Quaternary Science Reviews 21 (18–19), 2019–2046.